D E U T S C H E S E L E K T R O N E N - S Y N C H R O T R O N
(DESY)
Hamburg-Gr. Flottbek 1, Flottbeker Drift 56

Desy-Notiz A 2.72
Hamburg, January 4, 1961
M 8

W. Kern
K. Steffen

A 3 BeV/c Spectrometer with a sloped Window in the p-θ-Plane
(Preliminary Design)

1) Parameters of the System
are given in Fig. 1

The stepfunctions K(s) and $1/\varrho$ (s), representing the focussing and the deflecting properties of the system, respectively, are shown in Fig. A.

Total length of the system = 14,80 m.

Est. total power at 3 GeV/c and σ = 0,42 rad^{-1}: ~950 kW.

The deflecting magnet M has parallel entrance and exit faces; therefore, it produces no horizontal focussing, but a weak vertical focussing.

2) Apertures

The quadrupole apertures assumed are shown in Fig. 2.

Fig. 2

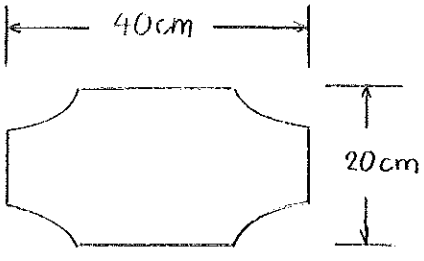

The aperture of the magnet M is 40 cm wide and 15 cm high.

In the quadrupol lenses, the area of the inscribed rectangular beam cross section is 400 cm^2. Due to the special shape of the lens aperture, the ratio of beam width to beam height is variable even within an individual lens between the limits 1 : 1 and 4 : 1.

3) Focussing Properties

x-component (horizontal):

An image of the target, magnified by a factor of four, is produced at point B in the magnet. Trajectories which are parallel in the magnet M are focussed into a point at the counter position C.

z-component (vertical):

An image of the target, demagnified by a factor 1/2, is produced at the counter position C.

These focussing properties are displayed in Fig. B, where a special particle trajectory is shown for each component.

4) Acceptances of the System for $\Delta p/p = 0$

Allowing, as we do, a sliding shape of beam cross section within lenses, the acceptances in horizontal and in vertical direction are coupled and cannot be computed independently any more. Choosing an acceptance $\varepsilon_z = 4 \cdot 10^{-4}$ [rad·m] for the vertical component and a beam envelope ($\tilde{z} \cdot \sqrt{\varepsilon_z}$) as shown in Fig. C, the maximum acceptance ε_x can be computed, observing the restrictions that $\tilde{x} \cdot \sqrt{\varepsilon_x}$ may not exceed 20 cm

and that the envelope product $\pi = (\tilde{x} \sqrt{\varepsilon_x}) \cdot (\tilde{z} \sqrt{\varepsilon_z})$ may not exceed 100 cm^2. The obtained emittances for both components at the target are shown in Fig. 3.

For the x-component, the inscribed parallelogram will be chosen as the beam emittance transmitted through the spectrometer. Its area $a = 8.10^{-3}$ [rad·m] corresponds to an emittance $\varepsilon_x = \frac{a}{\pi} = 25 \cdot 10^{-4}$ [rad·m] . Therefore, the acceptance product of the spectrometer is $\varepsilon_x \cdot \varepsilon_z = 10^{-6}$ [m^2·sterad]. The desired acceptance parallelogram will be precisely limited at all sides by defining slits, located at points A and D (Fig. 1). The two sides corresponding to $x' = \pm 83$ mrad will be limited by the slit at A, where particles emitted parallel at the target come to a focus. They will also be limited by the effective apertures of lenses Q 1 through Q 3, which are variable as described above and defined by the chosen vertical beam envelope $\tilde{z} \cdot \sqrt{\varepsilon_z}$. It is suggested to fill the lens openings outside of this effective aperture by an absorbing material, in order to reduce background of unwanted particles. The two other sides of the parallelogram are defined by the slit at D, where they appear vertical in the phase plane.

For the z-component, the ellipse of Fig. 3 will be replaced by a rectangle of equal area, orientation and ratio of axes. It will be defined by a limiting slit at E, where particles emitted parallel from the target come to a focus, and by the vertical dimension of the counters.

The transformations of the two components of the beam in the two phase planes are demonstrated in Fig. 4.

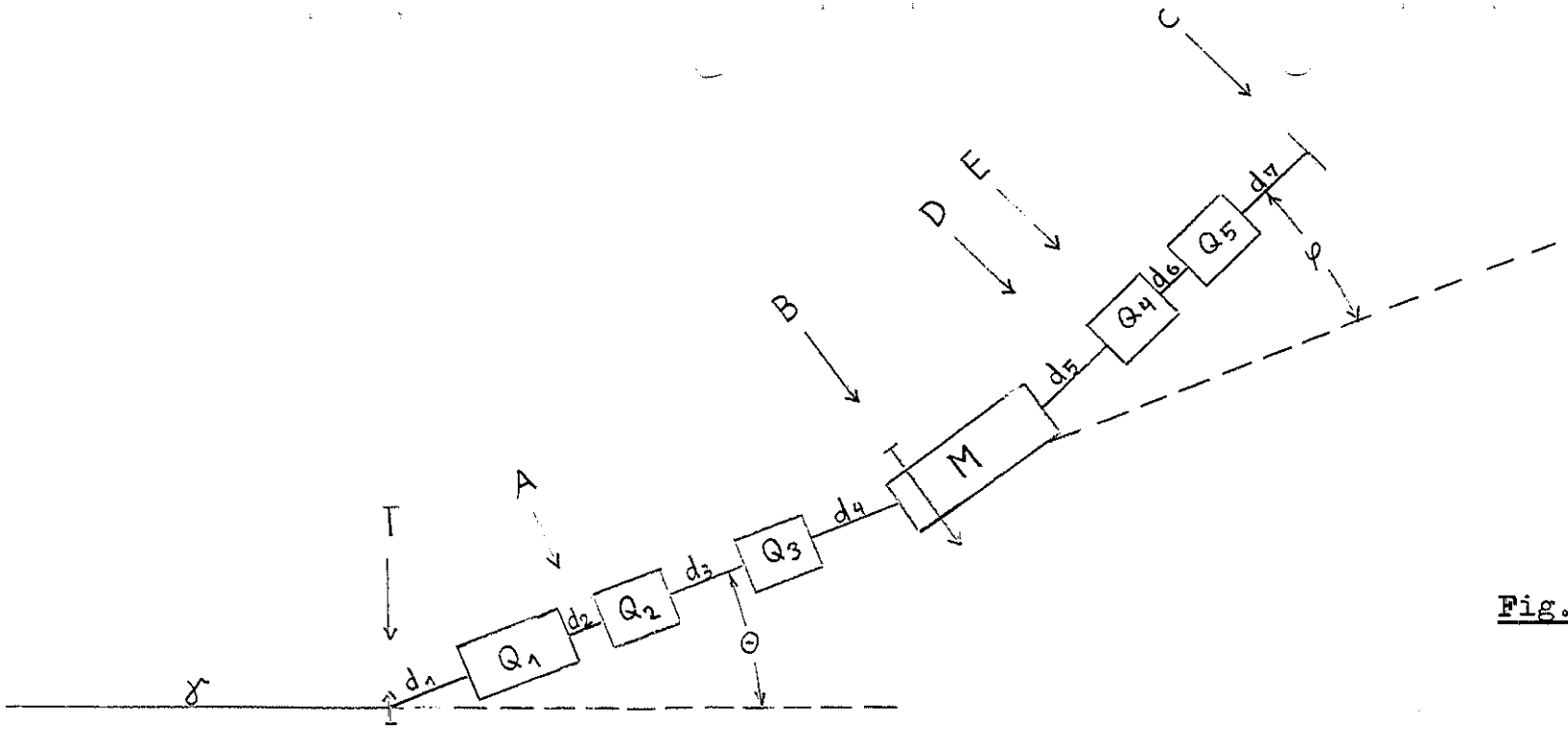

Fig. 1

	length [m]	K [m^{-2}]	1/ϱ [m^{-1}]	est. power [kW]
Q_1	1,50	+ 0,79		220
Q_2	1,00	- 0,79		160
Q_3	1,00	+ 0,43		50
Q_4	1,00	+ 0,48		60
Q_5	1,00	- 0,80		160
M	2,28		+ 0,178	300
			est. total power	950 kW

d_1 = 1,15 m
d_2 = 0,50 m
d_3 = 1,08 m
d_4 = 1,31 m
d_5 = 1,20 m
d_6 = 0,51 m
d_7 = 1,25 m

K = 1 ≙ 1 kΓ/cm
1/ϱ = 0,1 ≙ 10 kΓ
} at 3 BeV/c

Power assumptions:
Q: 5 kW/liter + 25 kW
M: 2,5 kW/liter + 15 kW
} for each end at { 1 kΓ/cm / 20 kΓ

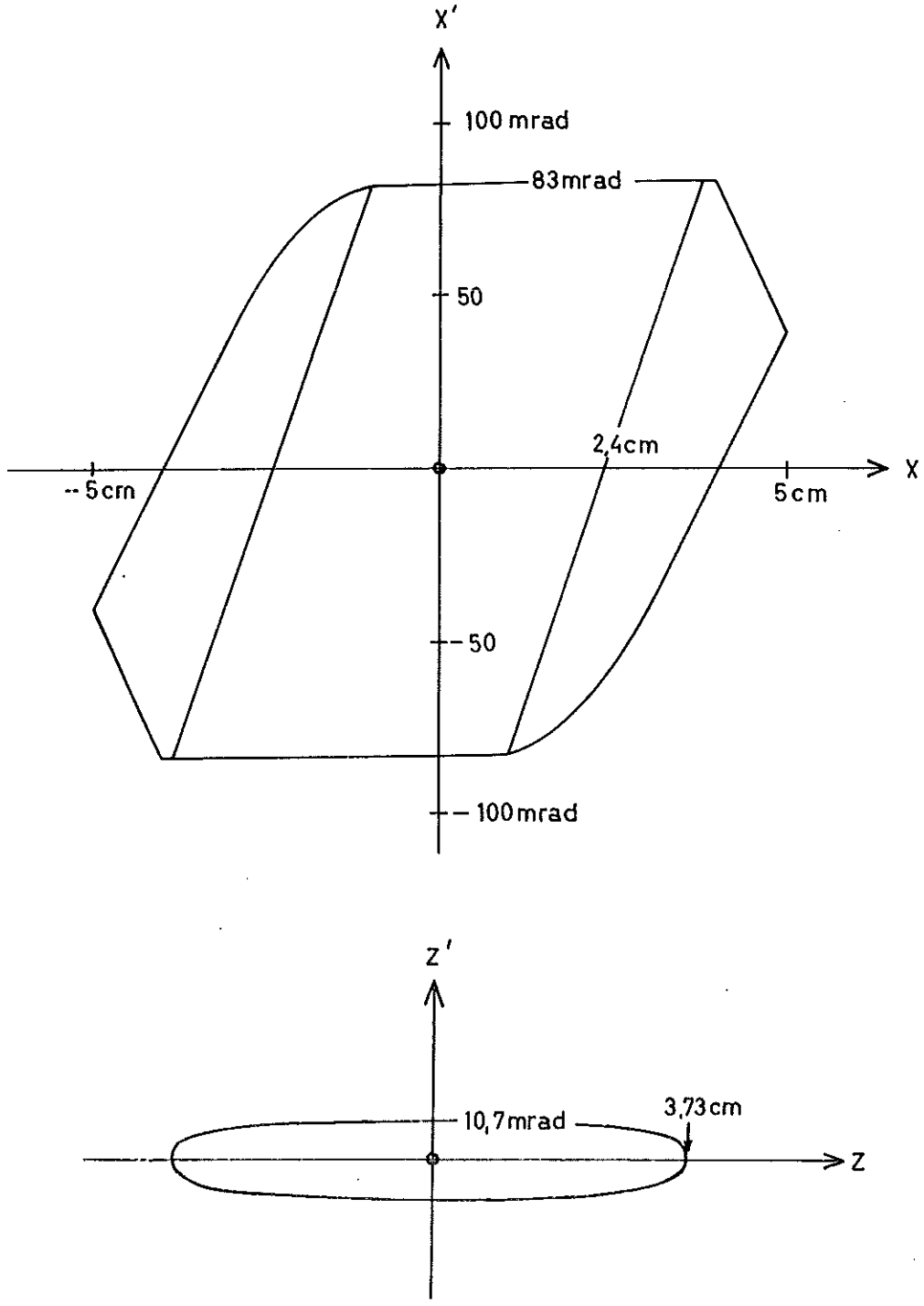
X'
100 mrad
83mrad
50
2,4cm
X
-5cm
5cm
50
100mrad
Z'
10,7mrad
3,73cm
Z

Fig. 3

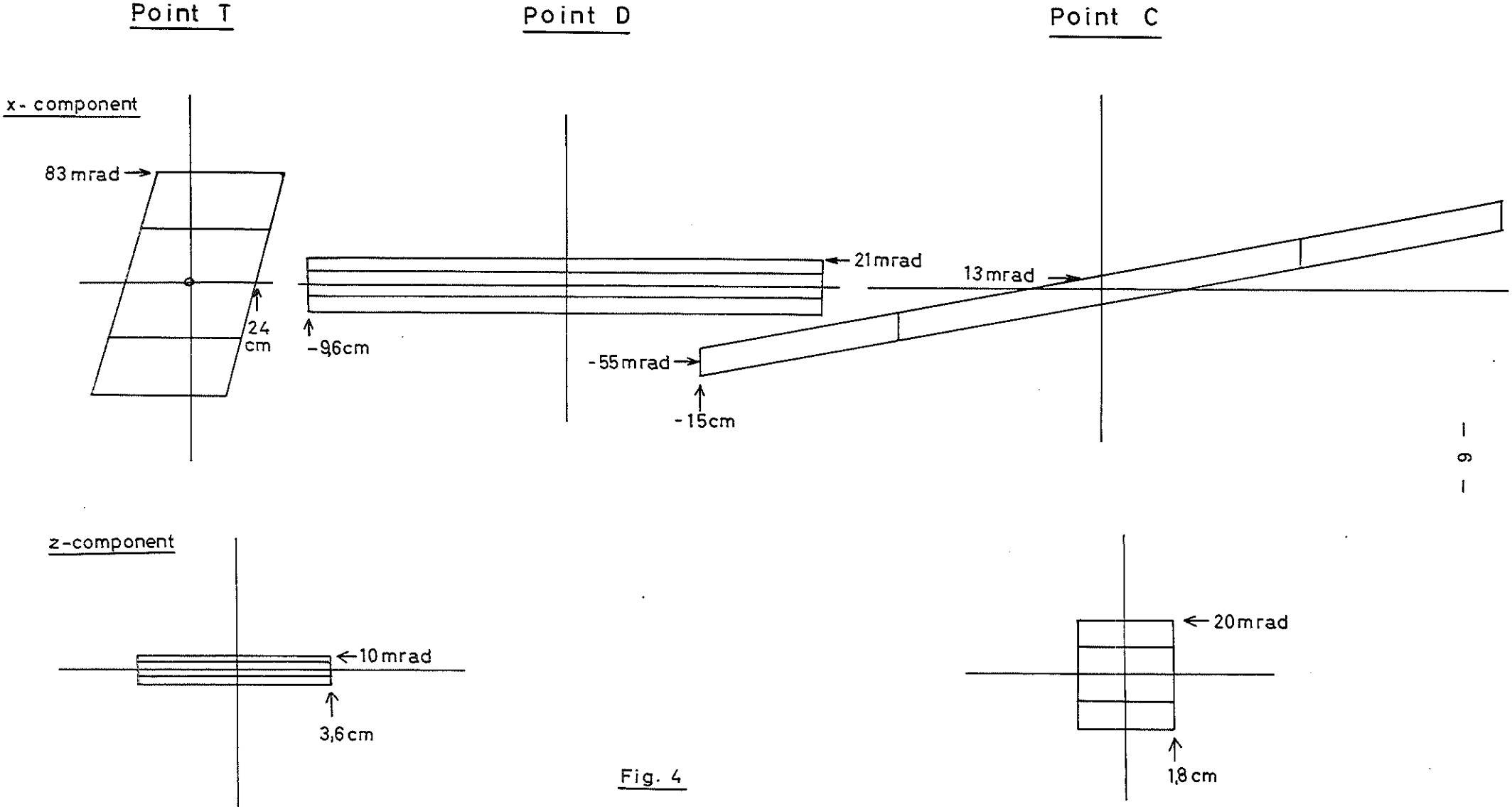
Point T
Point D
Point C
x - component
83 mrad
24 cm
-9,6cm
21mrad
13mrad
-55mrad
-15cm
z-component
10mrad
3,6cm
20mrad
1,8cm

Fig. 4

5) Effect of deflecting Magnet M:
Sloped Window in p,θ-Plane

The effect of the deflecting magnet M can be described in phase plane language as a constant vertical shift of all x,x'-phase points in the centre of the magnet. Thus, the resolution of the magnet is inversely proportional to the divergence of the beam. In order to obtain an optimum momentum separation in a sloped window spectrometer, the magnet should therefore be placed, where particles emitted parallel from the target are parallel again and where the beam width is large (see Fig. B).

The change in direction, which the magnet induces on a particle with $\frac{\Delta p}{p} \neq 0$, is transferred into a displacement at counter position C by the quadrupole doublet Q 4 - Q 5. This displacement is proportional to $\frac{\Delta p}{p}$ (see Fig. D). On the other hand an angular deviation x'_o at the target also produces a displacement at C, which is proportional to x'_o (see Fig. E). Therefore, all particles arriving at a certain point x on the counter are located on a straight line in the p-θ-plane, with θ being the angle of emission at the target (see Fig. 5).

The slope σ of this line, as given by

$$\sigma = - \frac{d}{d\theta} (\ln p)$$

is inversely proportional to the deflection angle φ of the magnet (see Fig. 1):

$$\frac{1}{\sigma} = \ell \cdot \varphi = \ell \cdot \frac{eBL}{p} .$$

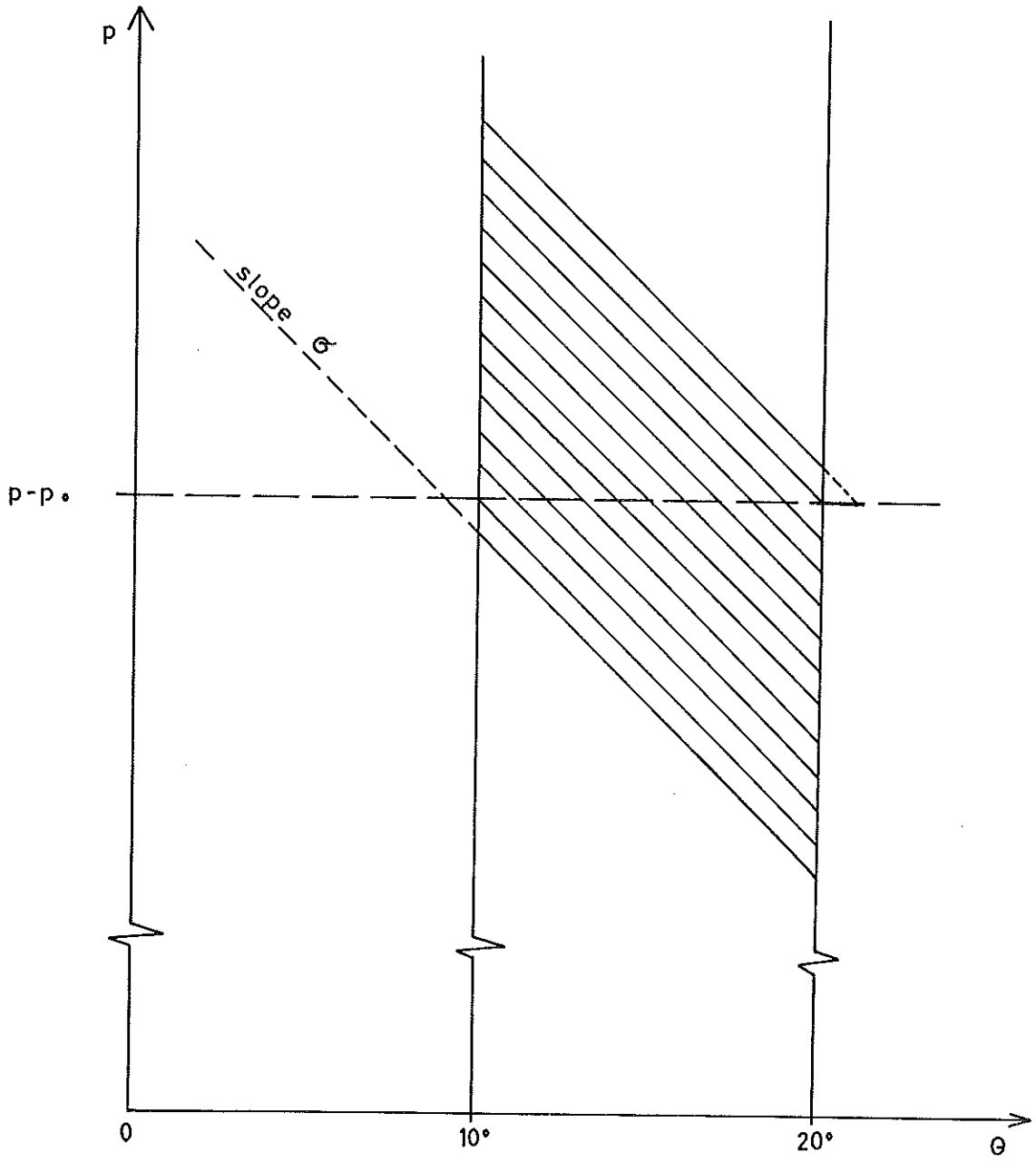

Fig. 5

The constant C is a figure of merit for the separating power of the system. In our case, $C = 6,0$. For the magnet parameters given above, i. e. for a maximum deflection angle $\varphi_{max} = 0,41$ rad $= 23,2^{o}$, this corresponds to a minimum slope

$$\sigma_{min} = 0,41.$$

However, there is enough space available to increase the magnet length to 3,50 m without changing the optical properties of the system. At the assumed field strength of 17,8 k Γ, the maximum deflection angle would then be $\varphi^{*}_{max} = 0,62$ rad $= 35,7^{o}$, and the minimum slope obtained

$$\sigma^{*}_{min} = 0,27.$$

In order to get a feeling for the significance of these figures, let us consider the observation of π^{+} from the reaction

$$\gamma + p \longrightarrow \pi^{+} + n.$$

In this case, the slope σ in the p,θ-plane can be adjusted parallel to the curve $E_{\gamma} = \text{const} = 3,2$ BeV down to observation angles

$$\theta_{min} \approx 7^{o} - 8^{o} \quad \text{for} \quad \sigma = 0,41$$

and $$\theta^{*}_{min} \approx 5^{o} - 6^{o} \quad \text{for} \quad \sigma = 0,27.$$

This seems to be quite sufficient, especially in view of the fact that such small observation angles might lead to difficulties for reasons of magnet geometry.

For a given momentum p and slope σ, one has for the deflection angle φ:

$$\varphi = \frac{1}{C \cdot \sigma}$$

for the magnetic deflection field B:

$$B = \frac{1}{e \cdot C \cdot L} \cdot \frac{p}{\sigma}$$

and for the field gradient g within lenses:

$$g = \frac{K}{e} \cdot p$$

Therefore, if one wants to set the spectrometer on a new momentum p and slope σ in the p,θ-plane, one has, in general, to change the fields as well as the deflection angle φ. Furthermore, the magnet M should always be aligned for symmetrical entrance and exit of the reference orbit (it might be possible to release this requirement; this will be investigated).

6) Transverse Dimensions of Counter Array

As may be seen from Fig. 4 or Fig. E, a total width of 30 cm is required for the counter array at point C in order to cover the full acceptance parallelogram in the x,x'-plane. The height of the counters must be 3,6 cm. The total counter area can be divided into an array of individual counters, each one covering a narrow interval

of energy E_o of the incoming particle. For instance one might choose 10 counters, each 3 cm wide. In the reaction $\gamma + p \longrightarrow \pi^+ + n$, each counter would then cover a strip in the p-θ-plane with "length" $\Delta\theta = 10^o$ and, at $E_o = 3$ GeV and $\theta_o = 15^o$, "width" $\frac{\Delta E_\gamma}{E_\gamma} \approx 1{,}5$ %.

A closer investigation of the system shows that the apertures of the lenses Q 4 and Q 5 allow to place additional counters 5 cm wide on each side of the counter array without having their "illumination" reduced by the lens apertures. It is therefore suggested to place one additional counter on each side. The total "sloped window" in the p,θ-plane accepted by the counter array in this case is shown schematically in Fig. 5.

7) Suggested Target Arrangement

Since for a sufficiently large target the intensity accepted by the spectrometer is difined by its acceptance only, we suggest to use a liquid hydrogen target which is transversally wider than the well collimated primary beam, and let the spectrometer itself select the effective target volume. The target can then be made very long, which results in a strong intensity increase for all observation angles θ not too far from the forward direction. The effective target volume is strongly dependent on θ in this case, but it can be computed with sufficient accuracy if the primary beam is well collimated.

8) Remarks on the Minimum Observation Angle θ min.

In order to have the primary beam clear the first lens Q 1, θ_{min} is limited by the width of its coil and return yoke.

A reduction of this width might be possible by using a Panofsky-type lens, cut into half, and adding a magnetic mirror on its open side. Then, Θ_{min} would be limited by the width of this magnetic mirror. Q 1 would in this case represent a lens with a superimposed deflecting field. A preliminary investigation shows that this additional deflecting field would not noticeably change the properties of the system, and on the other hand, would help to turn the direction of the spectrometer away from the primary beam direction.

Addendum:

It was pointed out to us by Dr. Meyer-Berkhout that an angular interval of $\Delta\Theta = 10^{o}$, as suggested in our design, might be too large in experiments requiring good angular resolution.

This difficulty could, however, be overcome by placing another array of counters at the position of slit A. By operating the counter arrays at A and C in a coincidence matrix, one would in effect further subdivide the acceptance area in the p,Θ-plane (see Fig. 5) into small angular intervals. Taking, for instance, 10 counters, each 1,7 cm wide and about 12 cm high, one would obtain a subdivision of the 10^{o} interval into ten strips of 1^{o} each.

The small-angle scattering of particles from the counters at A does not reduce the resolution of the spectrometer since an image of A is produced at C. The thickness of the counters at A must, however, be limited, because of momentum loss of particles. The momentum interval $\frac{\delta p}{p}$ accepted by each of the ten counters at C is

$$\frac{\delta p}{p} \cong \frac{1}{10} \sigma \cdot \Theta = 1{,}74 \cdot \sigma \ [\%]$$

Therefore, at σ = 0,41 : $\frac{\delta p}{p}$ = 0,72 %
and σ = 0,27 : $\frac{\delta p}{p}$ = 0,47 %

The momentum loss of particles in the counters at A should be small compared to these values. Therefore, this scheme can be used with all heavier particles, but will be difficult to be applied in the electron scattering experiment, because this would demand scintillators less than 1 mm thick. For photo production experiments, however, this design seems to combine high resolution and flexibility with a large acceptance.

Acknowledgements:

We would like to thank Dr. P. Stähelin, Dr. P. Joos and G. Sommer for interesting discussions stimulating this design. They first pointed out to us that in order to bend away from the primary beam direction one could place the deflection magnet behind a reversed image of the target.

Nomenclature:

s	coordinate along reference orbit
x horizontal, z vertical	coordinate transverse to ref. orbit
$x' = \frac{dx}{ds}$, $z' = \frac{dz}{ds}$	
x_o, x'_o; z_o, z'_o	Initial conditions of particle trajectories
$\hat{x}$	particle trajectory with $\frac{\Delta p}{p} \neq 0$, x_o and $x'_o = 0$
$\tilde{x}$ horizontal, $\tilde{z}$ vertical	beam envelope (phase plane ellipses assumed)
$\tilde{x}_o, \tilde{x}'_o$; $\tilde{z}_o, \tilde{z}'_o$	Initial beam conditions (phase plane ellipses assumed)
$K(s) = \frac{e \cdot g(s)}{p}$	$\varepsilon = \frac{1}{\pi} \cdot$ (area of phase ellipse)
$\frac{1}{\varrho(s)} = \frac{e \cdot B(s)}{p}$	
$\pi(s) = \tilde{x} \cdot \sqrt{\varepsilon_x} \cdot \tilde{z} \cdot \sqrt{\varepsilon_z}$	

Remarks on Fig. A through E

1 Oscilloscope Unit (O.U.) ≈ 1 cm on photograph
Abscissa = s; 1 O.U. = 2 m throughout
Ordinates: see individual figures

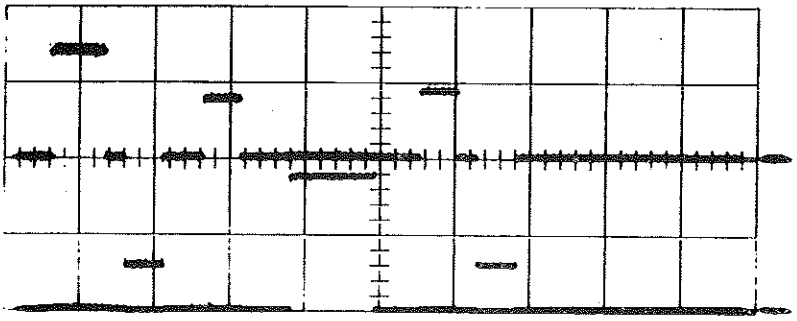

Figure A

K(s); 1 O.U. ≈ 0,5 m^{-2}; base line at centre of oscilloscope
$\frac{1}{\rho}$(s); 1 O.U. = 0,1 m^{-1}; base line at bottom

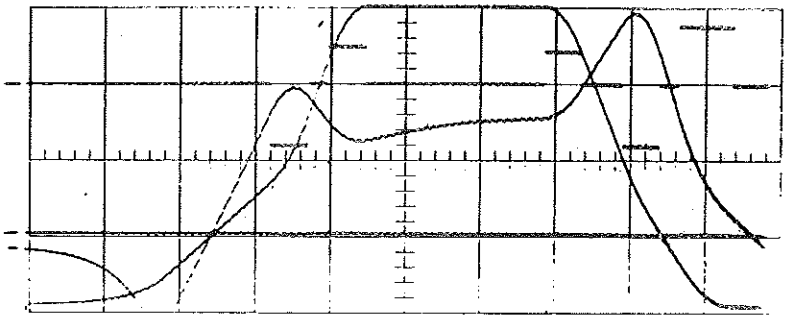

Figure B

K(s); 1 O.U. = 1 m^{-2}; base-line at 2nd line from top
x(s); x_o = -4,4 cm, x'_o = 0
z(s); z_o = 0 cm, z'_o = 21,6 mrad
} 1 O.U. = 5 cm, base line at 2nd line from bottom

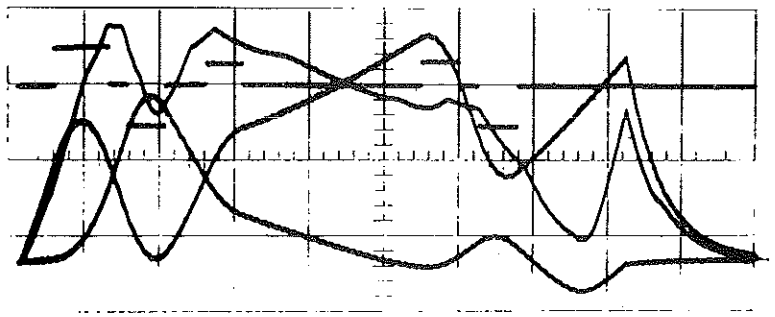

Figure C

K(s); not to scale, base line at 2nd line from top

$\tilde{x}(s)$; $\tilde{x}_o = 0{,}84\ m^{1/2}$; $\tilde{x}'_o = 0{,}88\ m^{-1/2}$; 1 O.U. = 5 cm at $\sqrt{\varepsilon_x} = 5 \cdot 10^{-2}\ m^{1/2}$

$\tilde{z}(s)$; $\tilde{z}_o = 1{,}87\ m^{1/2}$; $\tilde{z}'_o = 0\ m^{-1/2}$; 1 O.U. = 5 cm at $\sqrt{\varepsilon_z} = 2 \cdot 10^{-2}\ m^{1/2}$

$\pi(s)$; 1 O.U. = 25 cm^2 at $\begin{cases} \sqrt{\varepsilon_x} = 5 \cdot 10^{-2}\ m^{1/2} \\ \sqrt{\varepsilon_z} = 2 \cdot 10^{-2}\ m^{1/2} \end{cases}$

base line for $\tilde{x}$, $\tilde{z}$, π at bottom.

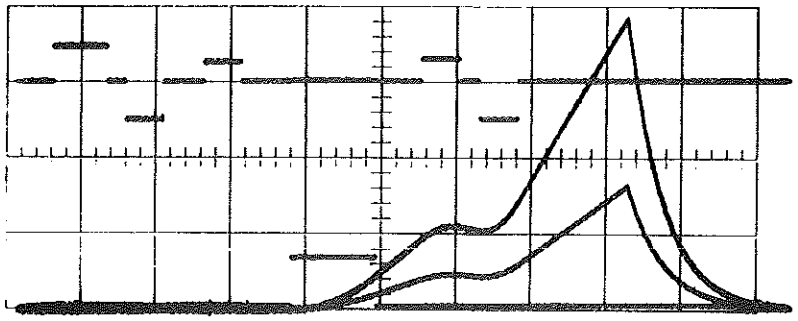

Figure D

K(s), not to scale, bare line at 2nd line from top
$\frac{1}{\rho}$(s), not to scale, base line at bottom
$\tilde{x}$(s), for $\Delta p/p$ = 2 % (lower curve) and 5 % (upper curve)
1 O.U. = 7,5 cm; base line at bottom

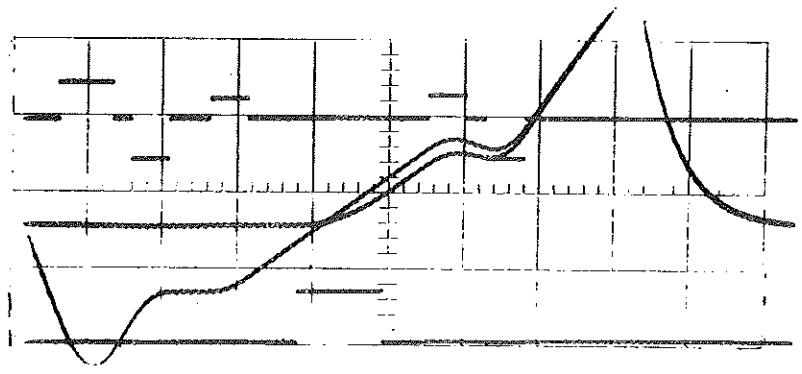

Figure E

K(s), not to scale, base line at 2nd line from top
$\frac{1}{\rho}$(s), not to scale, base line at bottom
$\hat{x}$(s), for $\Delta p/p$ = 2 %, 1 O.U. = 3,75 cm
x(s), x_o = 0 cm, x'_o = -48,3 mrad
base line for $\hat{x}$ and x between 2nd and 3rd line from bottom